

Anomalous Ferromagnetism of Monatomic Co Wire at the Pt(111) Surface Step Edge

Alexander B. Shick,¹ František Máca,¹ and Peter M. Oppeneer²

¹*Institute of Physics, ASCR, Na Slovance 2, CZ-182 21 Prague 8, Czech Republic*

²*Leibniz-Institute of Solid State and Materials Research, P.O. Box 270016, D-01171 Dresden, Germany*

(Dated: October 29, 2018)

A first-principles investigation of the anomalous ferromagnetism of a quasi-one-dimensional Co chain at the Pt(111) step edge is reported. Our calculations show that the symmetry breaking at the step leads to an easy magnetization axis at an odd angle of $\sim 20^\circ$ towards the Pt step, in agreement with experiment [P. Gambardella *et al.*, *Nature* **416**, 301 (2002)]. Also, the Co spin and orbital moments become noncollinear, even in the case of a collinear ferromagnetic spin arrangement. A significant enhancement of the Co orbital magnetic moment is achieved when modest electron correlations are treated within LSDA+*U* calculations.

PACS numbers: 75.30.Gw, 75.75.+a, 75.10.Lp

Exploring magnetism in the one-dimensional (1D) limit has been a great challenge for many years. Only recently, Gambardella *et al.* [1] succeeded to observe ferromagnetism of monatomic Co wires decorating the Pt(997) surface step edge. By exploiting the element-selectivity of the x-ray magnetic circular dichroism (XMCD), the existence of long-range ferromagnetic order on Co was demonstrated below 15 K [1, 2]. Although theoretically the Mermin-Wagner theorem [3] forbids long-range 1D ferromagnetic order at non-zero temperatures, ferromagnetism in 1D can be stabilized by a large magnetic anisotropy energy, which creates barriers effectively blocking thermal fluctuations. The significance of such blocking mechanism was recognized earlier for the occurrence of long-range magnetic order in 2D systems [4, 5].

The experiments of Gambardella *et al.* revealed novel magnetic properties of monatomic Co wires at Pt step edges. An unexpected magnetocrystalline anisotropy was observed: the easy magnetization axis was directed along a peculiar angle of $+43^\circ$ towards the Pt step edge and normal to the Co chain. The magnetocrystalline anisotropy energy (MAE) was estimated to be substantial, of the order of 2 meV/Co atom [1]. In addition, a considerable enhancement of the Co orbital magnetic moment $M_L \approx 0.7 \mu_B$ —as compared to the bulk Co M_L value of $0.14 \mu_B$ —was deduced from XMCD experiments.

In this paper we report a first-principles investigation of the anomalous ferromagnetism of a monatomic Co wire at the Pt(111) surface step edge, using state-of-the-art electronic structure calculations. We focus on the intriguing features of the quasi-1D Co wire, i.e., the easy axis rotated away from the (111) surface normal, the enhanced Co orbital moment and huge estimated MAE. The key outcomes of our study are (*i*) the *ab initio* calculation of an easy axis at an odd angle rotated towards the Pt step edge and (*ii*) the prediction of an intrinsic noncollinearity between spin and orbital magnetic moments of both the ferromagnetic Co wire and Pt substrate. The origin of this novel magnetic behavior, which is to our knowledge not present in known 2D and 3D

itinerant ferromagnets is explained to be a consequence of the magnetic symmetry lowering at the surface step edge [6]. Our calculations furthermore yield a MAE of the order of 4 meV/Co atom, and—using the LSDA+*U* approach—a Co orbital moment $M_L = 0.45 \mu_B$.

Previously, several computational studies of the magnetic properties of adatoms, clusters, and monatomic chains on surfaces were reported (see, e.g., [7, 8, 9, 10, 11]). The calculations predict in general an enhanced MAE closely related to the reduced dimensionality and enhancement of the orbital moment. However, in all of these studies only transition-metal wires or adatoms on *flat* surfaces are investigated, i.e., geometries that are essentially different from the metal wire at a step edge. For wires, adatoms or clusters [8] at flat surfaces the easy axis is either normal to the surface or in-line for some wires [11]. So far only one *ab initio* study of Co at a Pt step edge was reported, in which the XMCD spectrum was computed [12], but the magnetic anisotropy was not considered. Our study focuses on the unprecedented magnetic anisotropy properties observed for the quasi-1D Co chain.

Methodology. We performed supercell calculations to model the Co chain at the Pt(111) surface step edge. Supercells of various sizes were investigated. We shall discuss here particularly two supercells: one of small size, a toy model, which we name model I, and a large, realistic supercell, model II (see Fig. 1). Model I consists of one subsurface Pt layer built of 4 rows of Pt and one surface layer containing one row of Co atoms, two rows of Pt, as well as one empty row to model the step edge. Model II consists of a sub-subsurface and a subsurface Pt layer built of 6 rows of Pt atoms, while the surface step is modeled by 3 rows of Pt, one Co row, and two rows of empty Pt sites. In both supercells the vacuum is modeled by the equivalent of two empty Pt layers. All interatomic distances are adopted to be those of pure Pt. We note that while model II approaches the maximally treatable supercell size for full-potential, relativistic calculations of the MAE, the proportions of the experimental Co chain

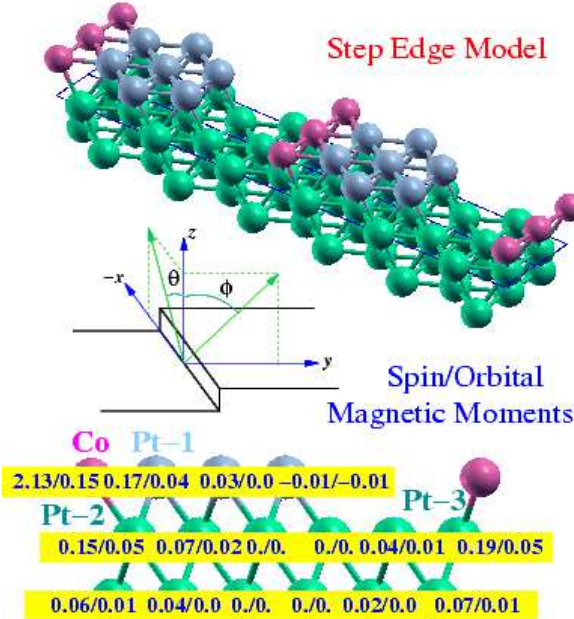


FIG. 1: Top: schematic crystal structure of model II, used to represent the Co chain at the Pt(111) surface step edge [13]. Middle: Definition of the angles θ , ϕ , and coordinate axes. The x axis is chosen parallel to $[1\bar{1}0]$ (along the Co wire), the y axis to $[1\bar{2}1]$ (normal to the wire), and the surface normal z is chosen parallel to $[111]$. Bottom: profile sketch with calculated M_S^z/M_L^z values specified.

at the Pt(997) step edge are still larger, consisting of an 8 Pt rows wide terrace at the Pt step [2].

The first-principles calculations were performed using the relativistic full-potential linearized-augmented-plane-wave (FP-LAPW) method, in which the spin-orbit coupling is included in a self-consistent second-variational procedure [14]. For most of the calculations the conventional (von Barth-Hedin) local spin-density approximation (LSDA) is adopted, which is expected to be valid for itinerant metallic systems. In order to capture better the electron correlations expected for the Co 3d electrons in the reduced dimension also the LSDA+ U approach, in the implementation of Ref. 15 has been applied. For further details of the calculations, see Ref. 16.

First-principles results. We first applied the conventional LSDA approach using the FP-LAPW method. To start with, the spin magnetization axis was chosen to be fixed either along the x , y , or z axis. The essential computed spin (\vec{M}_S) and orbital (\vec{M}_L) moments are given in Table I. Table I reveals that the \vec{M}_S and \vec{M}_L on Co and Pt are *noncollinear* for a spin moment fixed along the y or z axis, but *collinear* when \vec{M}_S is along the x axis. Non-collinearity of \vec{M}_S and \vec{M}_L has been predicted previously [17] for materials exhibiting a noncollinear spin magnetic

structure, but this is to our knowledge the first observation of such noncollinearity for a collinear, ferromagnetic spin configuration. To understand the noncollinearity of \vec{M}_S and \vec{M}_L it is instructive to consider the magnetic symmetry. The symmetry operations which preserve the crystal symmetry are the identity E and the mirror operation σ_x with respect to the yz plane (see Fig. 1). Considering now the magnetic symmetry operations, which are—for a total magnetic moment in the yz plane— E and $\sigma_x R$, with R the time inversion, we observe that these symmetry conditions impose $M^x=0$, but $M^y, M^z \neq 0$ without any restriction. Therefore there is no particular symmetry imposed direction in the yz plane which would force spin and orbital moment to be parallel. In other words, the magnetic symmetry in the yz plane is the same for all magnetization directions. Along the wire the situation is different: the magnetic symmetry operations E and σ_x , which conserve M^x , force $M^y=M^z=0$ and consequently, we must have $\vec{M}_L \parallel \vec{M}_S$ for a magnetization along the wire.

From Table I we further observe that both the Co spin and orbital moment are considerably enhanced with respect to the values for bulk hcp Co [18], as expected for a dimensionality reduction leading to a more atomic-like configuration. The calculated M_S and M_L of Co agree well with those of Ref. 12, where however only z axis collinear components of M_S and M_L were considered. The Co M_S does not change when the supercell is enlarged from model I to model II, but small changes in the orbital moments exist. Also, there is a sizable magnetization induced on the nearest neighbor Pt atoms, which is decreasing rapidly for the Pt atoms farther away (see Fig. 1). The size of supercell model II appears thus sufficient to separate the magnetic Co wires and to ensure the Pt magnetization decrease away from the step edge.

Next, we turn to the salient aspect of our investigation, the MAE calculations. We used the so-called “magnetic force theorem” to compute the MAE: starting from self-consistent charge and spin densities calculated for the

TABLE I: Spin and orbital magnetic moments in μ_B , calculated for the monatomic Co wire at the Pt(111) step edge, using the supercell models I and II.

Model I, axis	\vec{M}_S			\vec{M}_L		
	x	y	z	x	y	z
$\vec{M}_S \parallel x$ axis	2.129	0	0	.084	0	0
$\vec{M}_S \parallel y$ axis	0	2.128	0	0	0.065	0.032
$\vec{M}_S \parallel z$ axis	0	0	2.127	0	0.009	0.155

Model II, atom ^a	\vec{M}_S	\vec{M}_L				
	x	y	z	x	y	z
Co	0	0	2.127	0	0.011	0.149
Pt-1	0	0	0.168	0	0.005	0.044
Pt-2	0	0	0.146	0	0.003	0.046
Pt-3	0	0	0.194	0	0.005	0.052

^a \vec{M}_S parallel z axis

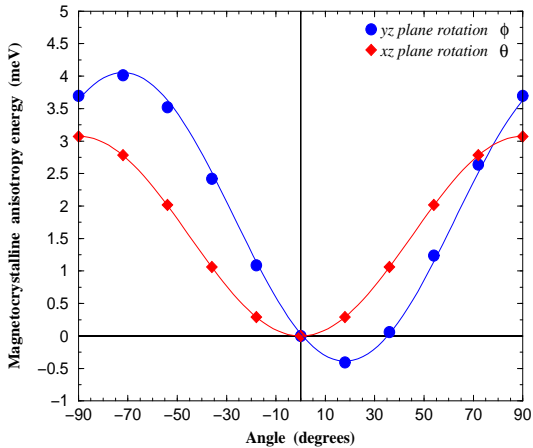


FIG. 2: The MAE calculated for model II as a function of the angles θ and ϕ of the spin moment. The solid lines are fits to the points and are given by $\text{MAE} = 4.04 - 4.44 \cos^2(\phi - 18^\circ)$ in the yz plane and $3.08 - 3.08 \cos^2 \theta$ in the xz plane.

spin moment aligned along the z axis, the M_S is rotated over angles θ or ϕ (see Fig. 1) and a single energy band calculation is performed for the new orientation of M_S . The MAE, which is defined as a directional total-energy difference, is computed from the change in one-electron energies E due to the M_S rotation, i.e., $\text{MAE} = E(\theta, \phi) - E(\theta = 0, \phi = 0)$ [19]. The calculated MAE is shown in Fig. 2 for supercell II.

For a rotation of M_S over an angle θ in the xz plane the MAE dependence on θ is symmetric, reflecting the mirror symmetry σ_x , with the easy axis pointing along the z direction and the hard axis directed along the Co wire. A MAE difference between the hard and easy axes of ~ 3 meV/Co (~ 1 meV/Co for model I) is calculated, exceeding by an order of magnitude the dipolar shape anisotropy [20].

For a rotation of M_S over an angle ϕ in the yz plane, we obtain a peculiar *asymmetric* dependence of the MAE on ϕ (see Fig. 2), reflecting the absence of any particular symmetry imposed direction in the yz plane. The computed easy axis is rotated away from the z axis by 18° towards the Pt step edge, in semi-quantitative agreement with the experimentally observed anomalous 43° easy axis [1]. The calculated direction of the hard axis of -72° corresponds reasonably with the experimental value of $\approx -50^\circ$ also. A notable difference appears for MAE calculations adopting model I: while the calculated $\text{MAE}(\phi, \theta = 0)$ curve is asymmetric as well, the minimum occurs at $\approx -50^\circ$ (not shown), thus oriented outwards from the Pt step. In contrast to supercell model II the toy model I is not valid even qualitatively for the MAE. Increasing the supercell size from model I to II improves the MAE, therefore an even better agreement with experiment can be expected for even larger supercells. The MAE difference between the hard and easy axes is ≈ 4.45

meV/Co for model II (≈ 1.6 meV/Co for model I), which is of the same magnitude as the experimentally estimated MAE of ~ 2 meV/Co at $T = 45$ K [1]. We expect a definitely higher experimental MAE and thus an even better agreement with model II for $T = 0$ K. We note that previous studies showed the conventional LSDA theory to be quite successful for describing the uniaxial MAE of hcp Co and CoPt bulk alloy [21, 22]. Here we demonstrate that the LSDA also provides a reasonable explanation of the MAE of the Co wire at the Pt step edge.

Although the LSDA works well for MAE calculations, it does not give large enough values for the orbital moment [18]. For example, the LSDA calculated M_L of hcp Co is with $0.08 \mu_B$ only half the experimental value of $0.14 \mu_B$. The situation is even worse for the Co wire. Comparing the LSDA calculated $M_L \sim 0.15 \mu_B$ (see Table I) with the experimental M_L of $0.68 \pm 0.05 \mu_B$ [1] indicates that the LSDA value is too small by a factor of 4.5! Recently, the orbital-polarization correction (LSDA+OP) was applied to a Co wire on Pt, leading to a Co M_L of $0.92 \mu_B$ [12], but this value overshoots the experimental data.

To improve the M_L one needs to account for electron-correlation effects beyond the conventional LSDA, which is currently a challenging problem of *ab initio* relativistic energy-band theory. To estimate this effect, we use here the *semi-model* but physically transparent LSDA+ U method, which was shown to correct the Co M_L of both hcp Co and CoPt alloy with a *single* choice of the Coulomb U ($= 1.7$ eV) and exchange J ($= 0.91$ eV) parameters [21]. Using the same U and J , we compute $M_L^z = 0.45 \mu_B$ for supercell II when M_S is along the z axis ($M_L^z = 0.32 \mu_B$ for model I). These values are still smaller than the experiment but we expect a larger M_L with a further increase of the supercell, due to a related Co d -states localization. We could of course obtain better agreement with experiment by another choice of U and J , but we prefer to use the “universal” values found in Ref. 21, treating thus the U of metallic Co as a transferable, atom specific quantity. The Co spin moment hardly changes, from 2.13 to $2.18 \mu_B$ when the U is included. We note, that in the LSDA+ U method the MAE can be computed only from total energies, as it is incompatible with the force theorem. It will require highly accurate self-consistent calculations for the M_S rotated over different angle θ and ϕ , something which is numerically not a practicable approach.

To understand how the enlargement of the Co M_L in the LSDA+ U approach comes about we consider the spin and orbitally resolved $3d$ densities of states (DOS) of model II, which are shown in Fig. 3. The spin-resolved LSDA DOS reveals a substantial narrowing of the band width from ~ 6 eV for hcp Co to ~ 4 eV for the Co wire as well as a moderate increase of the spin-splitting (Fig. 3a), as is expected for the reduced Co coordination. When the U is included the $3d$ DOS broadens somewhat and sig-

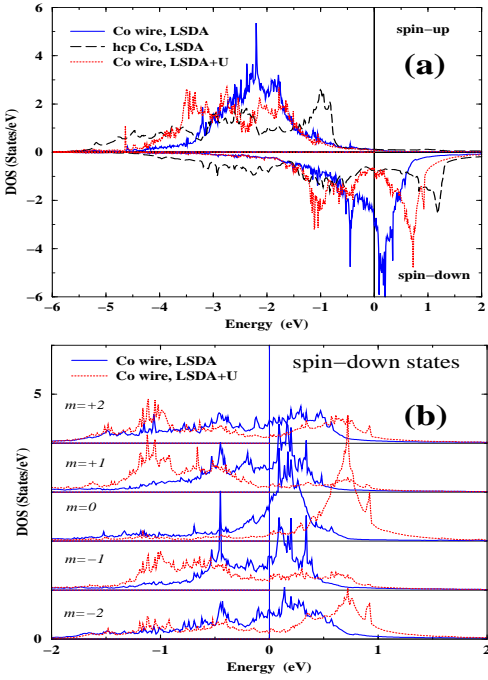


FIG. 3: (a) The spin-resolved 3d DOS, computed with the LSDA and LSDA+ U for model II, and compared with the LSDA DOS of hcp bulk Co. (b) The orbitally-resolved, spin-down DOS calculated with the LSDA and LSDA+ U methods.

nificant changes in the spin-resolved DOS occur. Since the spin-up Co d -band is fully occupied, only changes of the spin-down band are essential for the M_L enhancement. The spin-down m -resolved 3d DOS of the Co wire is shown in Fig. 3b. A major change in the LSDA+ U DOS appears as an upward shift within the $|\downarrow; m = 0\rangle$ DOS, which, however, does not contribute to M_L . The major contribution to the increase of M_L originates from an upward shift within the $|\downarrow; m = -2\rangle$ and a downward shift of the $|\downarrow; m = +2\rangle$ DOS. Also, downward shifts of the $|\downarrow; m = \pm 1\rangle$ states take place, but these contribute only secondarily to the M_L change. Thus, we conclude that the M_L enhancement with the Coulomb U is brought about by modifications of the in-plane spin-down $x^2 - y^2$ and xy orbital densities and much less affected by changes in the out-of-plane xz, yz , and $3z^2 - r^2$ orbital densities. The in-plane orbitals are affected most by the missing Pt atoms at one edge side and thus most liable to localize.

In conclusion, employing first-principles calculations we have provided a microscopic picture of the anomalous magnetocrystalline anisotropy of a quasi-1D Co chain at the Pt(111) step edge. The essential symmetry breaking at the step edge leads to noncollinear spin and orbital moments as well as to an easy magnetization axis oriented at a peculiar angle towards the Pt step edge. LSDA theory is found to provide a rather good explanation of the magnetocrystalline anisotropy, yet a consider-

able improvement of the Co orbital moment is obtained with LSDA+ U calculations.

We gratefully acknowledge discussions with P. Gambardella, P. Novák, H. Eschrig, and W.E. Pickett. This work was supported by the State of Saxony and the Grant Agency of the ASCR Grant A1010214.

- [1] P. Gambardella, A. Dallmeyer, K. Maiti, M. Malagoli, W. Eberhardt, K. Kern, and C. Carbone, *Nature (London)* **416**, 301 (2002).
- [2] P. Gambardella, *J. Phys.: Condens. Matter* **15**, 1 (2003).
- [3] N.D. Mermin and H. Wagner, *Phys. Rev. Lett.* **17**, 1133 (1966); P. Bruno, *Phys. Rev. Lett.* **87**, 137203 (2001).
- [4] J. Hauschild, H.J. Elmers, and U. Gradmann, *Phys. Rev. B* **57**, R677 (1998).
- [5] C.M. Schneider and J. Kirschner, in *Handbook of Surface Science*, edited by K. Horn and M. Scheffler (Elsevier, Amsterdam, 2000), p. 511.
- [6] Easy axes aligned at an angle to high-symmetry axes were reported previously for d -metal thin films [K. Baberschke and M. Farle, *J. Appl. Phys.* **81**, 5038 (1997)] and some $4f$ bulk materials [M. Colarieti-Tosti *et al.*, *Phys. Rev. Lett.* **91**, 157201 (2003)], and were explained by a competition of 2nd and 4th order MAE constants. This form of MAE is different from that of the Co-wire easy axis as it does not require the symmetry breaking.
- [7] J. Dorantes-Dávita and G.M. Pastor, *Phys. Rev. Lett.* **81**, 208 (1998).
- [8] I. Cabria, B. Nonas, R. Zeller, and P.H. Dederichs, *Phys. Rev. B* **65**, 054414 (2002).
- [9] D. Spišák and J. Hafner, *Phys. Rev. B* **65**, 235405 (2002).
- [10] B. Lazarovits, L. Szunyogh, and P. Weinberger, *Phys. Rev. B* **67**, 024415 (2003).
- [11] J. Hong and R.Q. Wu, *Phys. Rev. B* **67**, 020406 (2003).
- [12] M. Komelj, C. Ederer, J.W. Davenport, and M. Fähnle, *Phys. Rev. B* **66**, 140407 (2002).
- [13] The crystal structure is generated using XCrySDen [A. Kokalj, *J. Mol. Graphics Modeling* **17**, 176 (1999)].
- [14] A.B. Shick, D.L. Novikov, and A.J. Freeman, *Phys. Rev. B* **56**, R14259 (1997).
- [15] A.B. Shick and W.E. Pickett, *Phys. Rev. Lett.* **86**, 300 (2001).
- [16] In the self-consistent calculations we used 75 and 20 special k -points for model I and II, respectively, together with a Gaussian smearing. A quasi-2D Brillouin zone (BZ) with $k_z = 0$ was adopted in order to simulate the 2D-character of the problem, notwithstanding that the supercell calculations themselves are inherently three dimensional.
- [17] L.M. Sandratskii, *Adv. Phys.* **47**, 91 (1998).
- [18] J. Trygg, B. Johansson, O. Eriksson, and J.M. Wills, *Phys. Rev. Lett.* **75**, 2871 (1995).
- [19] We used 196 and 192 special k -points for model I and II, respectively, in a quasi-2D BZ with $k_z = 0$.
- [20] We estimate the dipolar anisotropy energy not to exceed ~ 0.1 meV/atom [cf. M. Eisenbach *et al.*, *Phys. Rev. B* **65**, 144424 (2003)].
- [21] A.B. Shick and O.N. Mryasov, *Phys. Rev. B* **67**, 172407 (2003).
- [22] P.M. Oppeneer, in *Handbook of Magnetic Materials*, Vol. **13**, edited by K.H.J. Buschow (Elsevier, Amsterdam,

2001), p. 229.